DEVELOPMENT OF A SHORT PERIOD CRYOGENIC UNDULATOR AT RADIABEAM*

F. H. O'Shea†, R. Agustsson, Y.-C. Chen, A. J. Palmowski, and E. Spranza,
RadiaBeam Technologies, Santa Monica, CA, USA

Abstract

RadiaBeam Technologies has developed a 7-mm period length cryogenic undulator prototype to test fabrication techniques in cryogenic undulator production. We present here our first prototype, the production techniques used to fabricate it, its magnetic performance at room temperature and the temperature uniformity after cool down.

INTRODUCTION

The goal of this project was to build a cryogenic undulator that used praseodymium-iron-boron magnets and textured dysprosium (TxDy) poles. The latter material is being developed at RadiaBeam using an in-house formula for production that shows a great deal of promise for increasing the gap field strength of short period undulators, while the magnets were purchased from a vendor. Both the material development and undulator design goals have been discussed in previous publications [1–4].

Because dysprosium's Curie temperature is approximately 90 K, the undulator is necessarily cryogenic. The choice of praseodymium based magnets is because of a spin-axis reorientation in neodymium magnets [5], and they are stronger than samarium cobalt magnets.

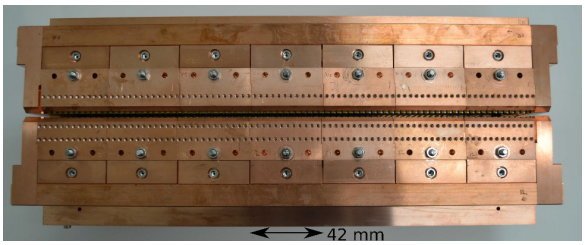

Figure 1: Image of the cryogenic undulator.

We met with much success in understanding the TxDy and have developed a strong understanding of the features of its performance. Unfortunately, we also had considerable difficulty attaining our desired level of batch-to-batch consistency in the textured dysprosium [2, 3]. Without regular access to a cryogenic hysteresisgraph or vibrating sample magnetometer the turn around time for sample production and testing made exploration of production parameters impractical. Eventually, we had to cease the development of the textured dysprosium.

While the TxDy was being developed, the undulator design became quite advanced and showed promise for functioning as a room temperature undulator using vanadium permendur (VP) poles. In order to test the engineering design of the undulator and take advantage of further development of the TxDy we hope to pursue in the future, we built a 42 period undulator using VP poles instead of TxDy. The undulator is shown in Fig. 1. The prototype undulator performed favorably compared to our desired specifications [1–4].

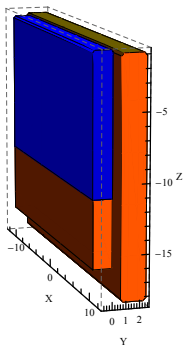

Figure 2: Layout of the minimum element representation of the undulator in Radia. The orange objects are permanent magnets and the blue object is the pole. The backing magnet can be seen below the pole. All axes have units of mm. The electron beam travels along the $\hat{y}$-axis at $x = z = 0$.

MAGNETIC DESIGN

The work discussed in the section was performed before the switch from TxDy to VP. It nonetheless describes the motivation for the design decisions made for the undulator that was produced.

We used Radia to design the undulator [6]. The Radia representation of the minimum magnetic element is shown in Fig. 2. The magnetic properties for the dysprosium were taken from a vibrating sample magnetometer measurement made on an initial sample [2]. The material properties for the magnets were taken from measurements of the hybrid praseodymium-neodymium based magnets available commercially [7]. The design gap of the undulator was fixed at 2 mm to allow access with a Hall probe.

A full design study was performed including managing demagnetization (or lack thereof), magnetic and mechanical tolerances and magnetic field strength optimization. The results for the dimensions and tolerances of the magnetically active objects is shown in Table 1. The low initial permeability of TxDy ($\mu_i \sim 10^2\mu_0$) as compared to VP

* Work supported by DOE under contracts DE-SC0006288 and NNSA SSAA DE-NA0001979.
† oshea@radiabeam.com

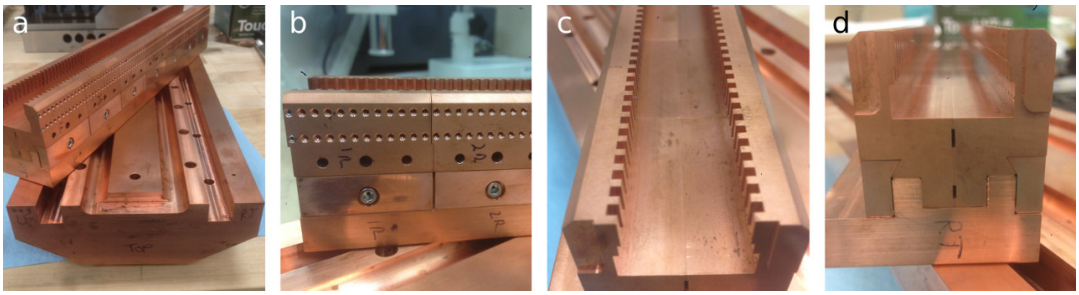

Figure 3: Various views of the copper structure of the undulator during construction. (a) A jaw without magnets and poles sitting on top of the main strong back. (b) Close-up view of the modules fastened to the rail to form a jaw. (c) Close-up view of the modules showing the tabs in the modules used to restrain the poles (d) End view of a jaw showing the split module design and the dovetail clamps used to restrain the modules.

($\mu_i \sim 10^4 \mu_0$) combined with the high saturation induction of the material resulted in the decision to use backing magnets to increase the field strength on the magnetic axis. To minimize engineering complexity, we did not consider any "3D" designs such as side magnets or non-rectangular magnets or poles [8].

Table 1: Dimensions and tolerances for the placement and orientation of the poles and magnets. The tolerances for the backing magnets were not simulated. Axes are as defined in Fig. 2.

Dim.	Poles	Main Mag.	Back Mag.
x (mm)	21.0±0.1	24.5±0.1	24.5
y (mm)	1.45±0.05	1.95±0.04	1.35
z (mm)	11.0±0.1	17.4±0.025	6.9
θ_x (mrad)	0±9.5	0±4.5	N/A
θ_y (mrad)	0±2.3	0±2.5	N/A
θ_z (mrad)	0±5.7	0±4.0	N/A

Because of the difficulty in producing the textured dysprosium of the consistent quality needed for an undulator, we decided to create a prototype undulator using vanadium permendur poles instead of textured dysprosium. We did not include any end compensation scheme because this is an engineering design (not a production device) and we were focused on the main field nor did we perform magnet sorting. There are well known solutions to these problems in fixed gap undulators [9].

The substitution of the VP for TxDy had no ill-effect on the undulator design. In fact, because of the high permeability of the VP, the coercive fields in the magnets was reduced at all operating points. On the other hand, because the saturation induction is lower than that of TxDy, the simulated field strength on axis was reduced from 1.33 T to 1.23 T ($K = 0.8$) at 30 K.

MECHANICAL DESIGN

The structure of the undulator is split in to 3 levels: the main strong back seen at the bottom of Fig. 3a, the rail (seen at the bottom of Fig. 3d) and the modules (seen at the bottom of Fig. 3b and c). The modules are clamped to the rail by a pair of dovetail clamps and held in place horizontally on the rails by end plates (shown in Fig. 1). The combination of one rail, 7 modules and end plates is referred to as a jaw. The jaws are fastened in to the main strong back using precision machined slots in which the rails fit.

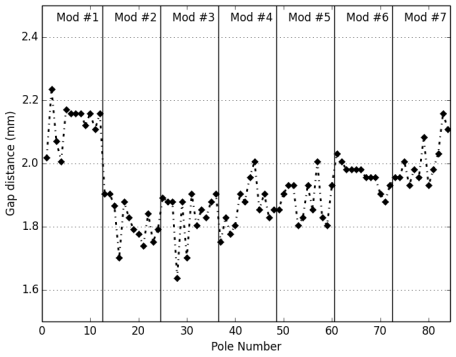

Figure 4: The total gap between each of the poles in the undulator. Each of the modules is labeled 1 through 7.

We used a calibrated theodolite to measure the distance of the poles from each other on the open side of the undulator, the result is shown in Fig. 4. The mean gap is 1.87±0.08 mm and there is a taper from one end of the undulator to the other. The mean gap is 0.13 mm smaller than the targeted value. This was caused by an improperly sized jig during trimming of the poles that resulted in the poles being larger in the $\hat{z}$-direction than desired. Further, review of the engineering drawings showed that several of the gap-defining features were allowed to vary (within tolerance) enough to account for the taper in the gap.

FIELD MEASUREMENT AT ROOM TEMPERATURE

The magnetic field of the undulator was measured at room temperature using a 1D Lakeshore 460 Hall probe and 460 Gaussmeter. The probe was secured to a 5-axis motion

system while the undulator was fastened to a 6-axis motion system. The probe was set to measure the field in the $\hat{z}$-axis. What little motion was possible in this direction was used to minimize the field measured at both ends of the undulator. The same procedure was used to minimize the field by moving the probe along the $\hat{x}$-axis. The two points found at either end of the undulator using this method defined the magnetic axis. A central line out along the magnetic axis was taken (see Fig. 5).

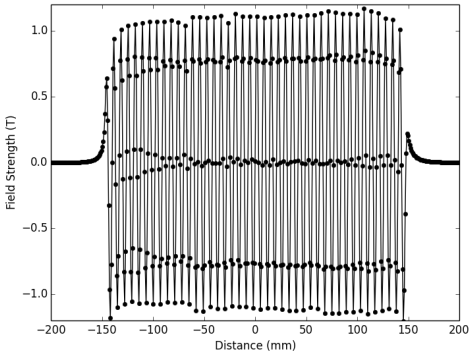

Figure 5: Plot of the data points taken during a line out scan along the magnetic axis of the undulator (circles) and a line connecting those points.

We found that the peak field in the central region of the undulator at room temperature is 1.11 ± 0.03 T (1.11 T in simulation) while the effective field is 1.10 T (1.12 T in simulation). The standard deviation of the peak field is 2.7%. When we correct for the previously discussed gap taper, the standard deviation is reduced to 1.4%.

We have tracked a 1 GeV electron through the magnetic field using a simple Euler's method explicit step routine. The uncorrected trajectory shows a strong linear walk-off of the electron from the axis. This is corrected in the tracking by adding a DC magnetic field to ensure that the electron beam exits the undulator on-axis. The root mean square (rms) phase error for the central region of the undulator is 11.1°.

There is a strong correlation between the gap measurement and the field strength (product-moment correlation coefficient of 0.8), indicating that a fraction of the phase error can be eliminated if the gap taper is corrected. After correcting for the taper the rms phase error for the central region of the undulator is 7.1°.

CRYOGENIC PERFORMANCE

The cryogenic performance of the undulator is shown in Fig. 6. Because of extreme space constraints in the test chamber, the cold head had to be installed horizontally which resulted in a significant drop in performance of the single stage cold head which had previously been cooled to below

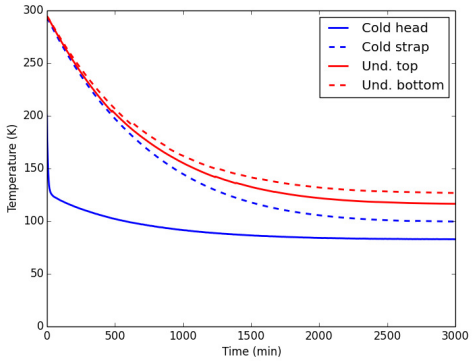

Figure 6: Temperature of the cryogenic test setup.

40 K. The temperature gradient along the length of the undulator was 10 K, which we attribute to incomplete thermal isolation of the undulator because the part of the undulator closest to the stand is the warmest.

REFERENCES

[1] R. Agustsson, Y.-C. Chen, T. Grandsaert II, A. Murokh, V. Solovyov, and F. O'Shea in *Proc. 3rd Int. Particle Accel. Conf. (IPAC'12)*, New Orleans, LA, USA, May 2012, paper MOPPP086, pp. 756–758.

[2] F. H. O'Shea *et al.*, in *Proc. 4th Int. Particle Accel. Conf. (IPAC'13)*, Shanghai, China, May 2013, paper WEPWA081, pp. 2298–2300.

[3] F. H. O'Shea *et al.*, in *Proc. 25th North American Particle Accel. Conf. (NAPAC'13)*, Pasadena, CA, USA, September 2013, paper THPAC36, pp. 1217–1219.

[4] A. Murokh *et al.*, *Nucl. Instr. Meth. A*, vol. 735, pp. 521–527, 2014.

[5] C. Benabderrahmane *et al.*, *Nucl. Instr. Meth. A*, vol. 669, pp. 1–6, 2012.

[6] P. Elleaume, O. Chubar, and J. Chavanne, in *Proc. 17th Particle Accel. Conf. (PAC'97)*, Vancouver, BC, Canada, May 1997, pp. 3509–3511.

[7] K. Uestuener *et al.*, in *Proc. of the 20th Workshop on Rare Earth Permanent Magnets and Applications*, Crete, Greece, July 2008.

[8] J. Bahrdt *et al.*, in *Proc. 33rd Int. Free Electron Laser Conf. (FEL'11)*, Shanghai, China, August 2011, paper THOAI1, pp. 425–432.

[9] J. A. Clarke, *The Science and Technology of Undulators and Wigglers*. Oxford, UK: Oxford University Press, 2004.